Viewing dark matter with weak gravitational lensing from HST

© **Richard Massey** [1,2]

[1] California Institute of Technology, 1200 E. California Blvd., MC 105-24, Pasadena, CA 911125, USA
[2] Institute for Astronomy, Royal Observatory, Blackford Hill, Edinburgh EH9 3HJ, UK
Email: rjm@astro.caltech.edu

Abstract: Ordinary baryonic particles (such as protons and neutrons) account for only one-sixth of the total matter in the Universe. The remainder is a mysterious "dark matter" component, which does not interact via the electromagnetic force and thus neither emits nor reflects light. However, evidence for its gravitational influence is mounting. The past few years have seen dramatic progress in measurements of weak gravitational lensing, the slight deflection of light from distant galaxies due to the curvature of intervening space. Recent observations from the Hubble Space Telescope have provided direct proof for, and large-scale maps of dark matter in the Universe. We review recent results, then prospects and challenges for future measurements of gravitational lensing from space.

1. Introduction

The concordance cosmological model poses a practical problem for observational astronomy. Mounting evidence from many quarters now suggests that five sixths of the material in the universe consists of exotic "dark matter" outside the standard model of particle physics. In particular, this dark matter is required not to interact via the electromagnetic force, and can therefore neither emit, reflect nor absorb light of any wavelength. Traditional modes of astronomical observations are thus rendered blind.

On the other hand, dark matter is expected to interact via gravity. Itcontributes to the slowing of the universe's expansion out of the big bang, and assists the accumulation of matter into the growth of large-scale structure. This interaction is also its giveaway: dark matter can be found and studied more locally via its gravitational influence on visible particles. The most direct technique, known as "gravitational lensing" studies the deflection of photons from distant galaxies as they pass through gravitational fields along our line-of-sight. This gravitational deflection, for example around massive galaxies or clusters of galaxies, is analogous to the deflection of light rays as they enter an ordinary glass lens with a refractive index different to that of air. The net deflection of light is of little observational use, because the galaxy cannot be viewed in the absence of lensing, so its original position is unknown. However, if opposite sides of a resolved image are deflected by different amounts, its image appears distorted.

When the distortion is strong, objects no longer resemble a galaxy, and the apparent shapes of individual galaxies can be used to infer the foreground gravitational field. An example of *strong gravitational lensing* around a massive galaxy cluster is shown in figure 1. However, most lines of sight through the universe do not pass near a massive galaxy cluster with a strong gravitational field. Farther out from the dense cores of clusters, the distortion is too small to be seen by eye, and first order assumptions of *weak gravitational lensing* become valid. In the weak limit, the image appears sheared, typically changing the axis ratio of galaxies by a few percent. Although it is impossible to measure this effect on individual galaxies, because their unlensed shapes are unknown, it is still possible to statistically detect the effect upon an ensemble collection of ~100 galaxies; even galaxies on adjacent lines of sight are usually at different redshifts, so physically far apart. Their true shapes must therefore be uncorrelated, and average to a circle in the absence of gravitational lensing. However, the shear signal is correlated over angular separations up to a few arcminutes, so that intrinsically circular shape becomes elongated into an observed ellipse. Noise on this measurement is dominated by the intrinsic shapes of the averaged galaxies, and about 100 galaxies are required because the typical distribution of galaxy shapes happens to bring the signal to noise on a measurement of their average ellipticity to unity.

To infer the distribution of foreground mass from measurements of weak gravitational lensing, the shapes of many thousands of distant galaxies are measured, and averaged on the sky into bins. Patterns in their mean ellipticites are then sought. As illustrated in figure 2, mass overdensities in front of the galaxies, such as galaxy clusters, produce a tangential "*E*-mode" pattern that is reminiscent of the tangentially-aligned strong lensing arcs. Foreground mass underdensities or voids produce radial "*E*-mode" patterns. Usefully, there is also an additional degree of freedom in the pattern of ellipticities. Curl-like "*B*-modes" are not produced by physical gravitational lensing. However, noise and most instrumental systematics are equally likely to occupy both modes. The measured *B*-mode signal can therefore act as an independent realisation of noise and a warning indicator for residual, uncorrected systematic effects in the desired *E*-mode.

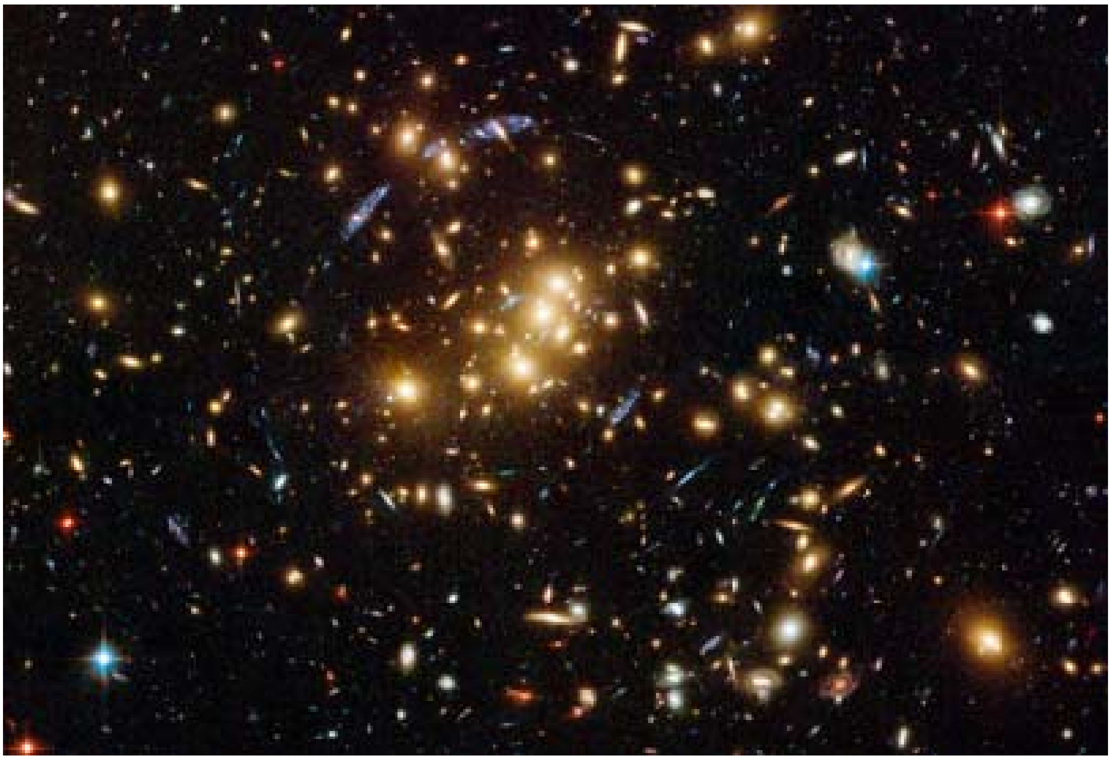

Fig. 1 Strong gravitational lensing around galaxy cluster CL0024+17, demonstrating at least three layers projected onto a single 2D image. The plus-shaped objects are nearby stars in our own galaxy; these are needed to model the telescope's point spread function. comparison of Eq.2 (dotted curve) with the observation data (filled circles) for supernovae of SNe Ia type [2]. The yellow, elliptical galaxies are members of the cluster, all at a similar redshift and gravitationally bound. Also amongst this group of galaxies is a halo of invisible dark matter. The elongated blue objects are much more distant galaxies that happen to lie behind the galaxy cluster . These are not physically associated with the cluster, but note their shapes. Gravitational lensing has distorted the images we see, producing a series of blue tangential arcs. Figure credit: NASA/ESA/M.J. Jee (John Hopkins University).

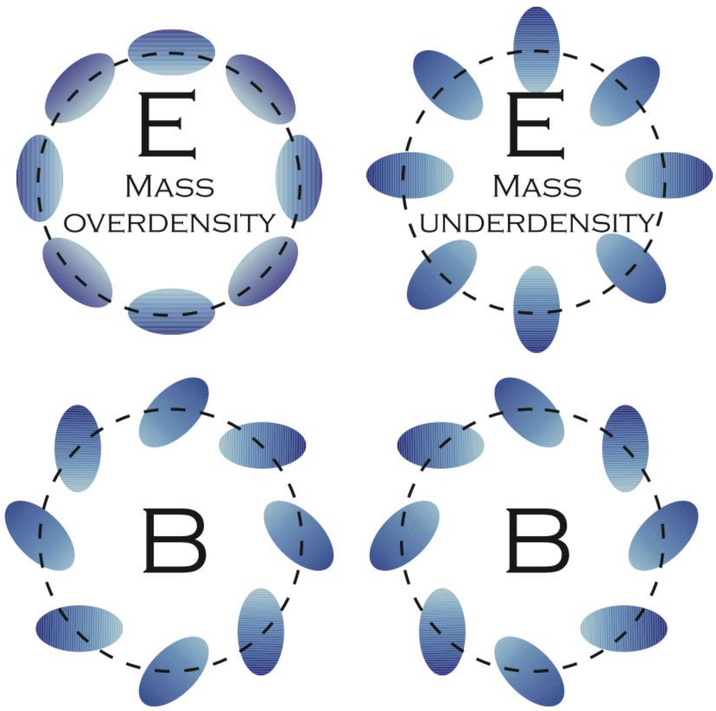

Fig. 2 The statistical signals sought by measurements of weak gravitational lensing are slight but coherent distortions in the shapes of distant galaxies. A tangential, circular pattern is produced around a foreground mass overdensity, reminiscent of the tangential arcs of strong lensing. On much larger scales (and much less pronounced, because the density contrast is limited), an opposite, radial pattern in the shapes of distant galaxies is produced by foreground voids. Physical gravitational lensing produces only these "*E*-mode" patterns. However, there is another degree of freedom in a shear (vector-like) field, and spurious artefacts can typically mimic both. Measurements of "*B*-modes" therefore provide a free test for residual systematics.

2. Instrumental nuisances

Although the weak lensing shear signal is coherent across several arcminutes, it is still weak. Measuring the tiny distortions in the shapes of distant (therefore small and faint) galaxies requires unusually precise control over imaging quality. For example, the galaxies are inevitably viewed after convolution with the telescope's Point Spread Function (PSF). For ground-based telescopes, this is dominated by turbulence in the Earth's atmosphere, and is particularly troublesome. Indeed, high precision weak lensing analysis will inevitably require wide-angle survey cameras in orbit. But even from space, diffraction through the finite aperture of the primary mirror blurs the shapes of small galaxies in a manner that can mimic or dilute a weak gravitational lensing signal. Hubble's low-Earth orbit also brings that telescope in and out of the shadow of the Earth; thermal expansions and contractions of only a few microns in its 13m length put it sufficiently out of focus to alter the ellipticity of the PSF, and consequently that of galaxies, by an amount comparable to the weak lensing signal. It is therefore necessary to model the shape of the PSF from stars within each image. Unusually for extra-galactic observations, the ideal sky location for a weak lensing survey is therefore at mid-galactic latitudes rather than the poles.

The current generation of cameras aboard Hubble also suffers from a second instrumental problem. Harsh radiation damage in orbit has damaged the CCD detectors, creating charge traps within the silicon substrate. At the end of each exposure, as the photoelectrons are transferred to the CCD readout register, these temporarily captured and only released after a short delay. Typically, the remaining photoelectrons have been transferred several more pixels by the time the captured electrons are released. The captured electrons therefore end up in a trail behind each astronomical object, adding a spurious ellipticity. This is a non-linear process, affecting faint and small galaxies more than bright, large ones: it therefore mimics the weak lensing signal. Worse still, because of the particular orientation of the two CCDs in HST's Advanced Camera for Surveys, the trails produce a spurious ellipticity signal that is confined to the *E*-mode. Current solutions include the empirical calibration of the spurious induced ellipticity as a function of galaxy size and flux. A great deal of additional effort is being invested in improved designs for hardware and basic data reduction software for future surveys.

3. Observations

3.1 Large-scale structure

The Hubble Space Telescope COSMOS survey (Scoville et al. 2007) is almost as deep as the Hubble Deep Field, and the largest optical survey ever obtained from space. At 2 square degrees, and containing two million galaxies, it was designed to contain a contiguous volume of the universe at redshift z=1 containing even the largest expected structures and at least one example of every type of environment. The single-colour HST imaging is backed up by ground-based spectroscopy of ten thousand (and growing) galaxies, plus multi-colour imaging at nearly fifty other wavelengths, from radio, through IR with Spitzer, optical, UV with Galex and X-ray with both Chandra and XMM. As well as accurate measurements of the shapes of galaxies, their (photometric) redshifts are also well understood. The X-ray imaging is also sensitive to hot gas, typically found within dense clusters of galaxies.

Figure 3 shows the observed ellipticities of half a million distant galaxies in the COSMOS field, corrected for convolution with the PSF and for CTE trailing. Several regions exhibit the circular patterns discussed above. Radial patterns are also present on larger scales, but are much less pronounced because the density contrast in a void is limited by the inability of mass to ever be less than zero. A filter to detect the patterns shown in figure 2 has been run over this data, and the measured *E*-mode signal is presented in figure 4. Contours show the reconstructed distribution of foreground mass: its filamentary structure is apparent. Interesting features include not only the concentrated mass peaks at the vertices of filaments, but also the completely empty voids. The coloured background depicts various tracers of baryons. The correlation between baryonic mass and total mass is striking. If the missing mass really does consist of dark matter particles that still interact via gravity, it is natural that they would end in the same place via their mutual gravitational attraction; in general throughout the universe, it appears that the dark matter forms a scaffolding around baryonic material.

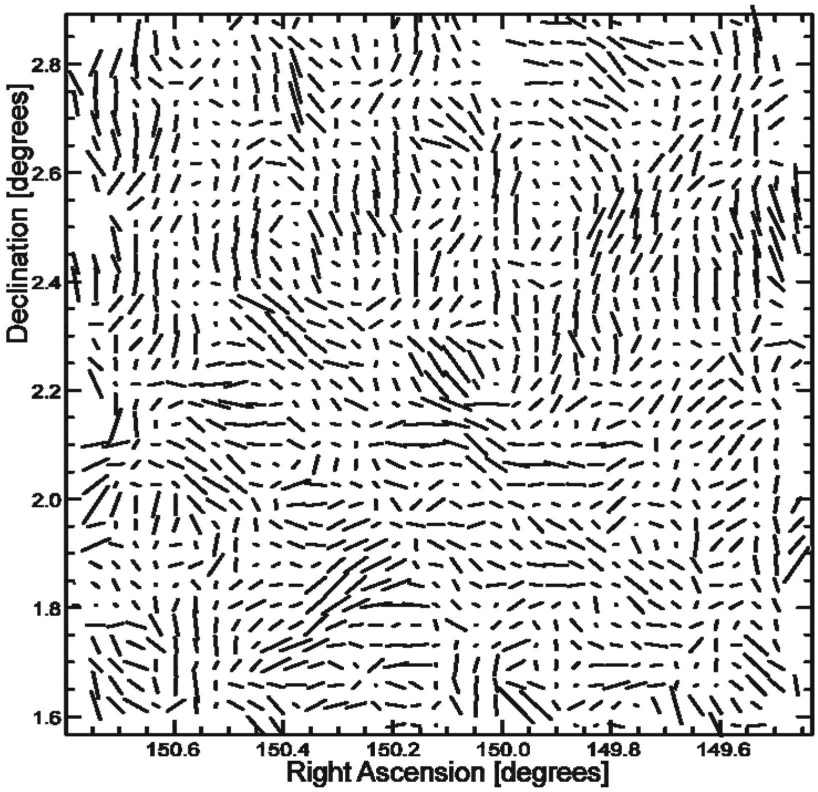

Fig. 3 The observed pattern of coherent ellipticity in background galaxies within the 2 square degree HST COSMOS survey. To improve visibility of the pattern, each tick mark represents the mean ellipticity of several hundred galaxies; the final analysis uses smaller bins containing about 80 galaxies and improves spatial resolution but adds noise. A dot in this plot represents a circular mean galaxy. Lines represent elliptical mean galaxies, with the line in the direction of the major axis and the length of the line proportional to the ellipticity. The longest lines represent an ellipticity of about 0.06. Several circular patterns are evident in this figure, such as that around (149.9, 2.5).

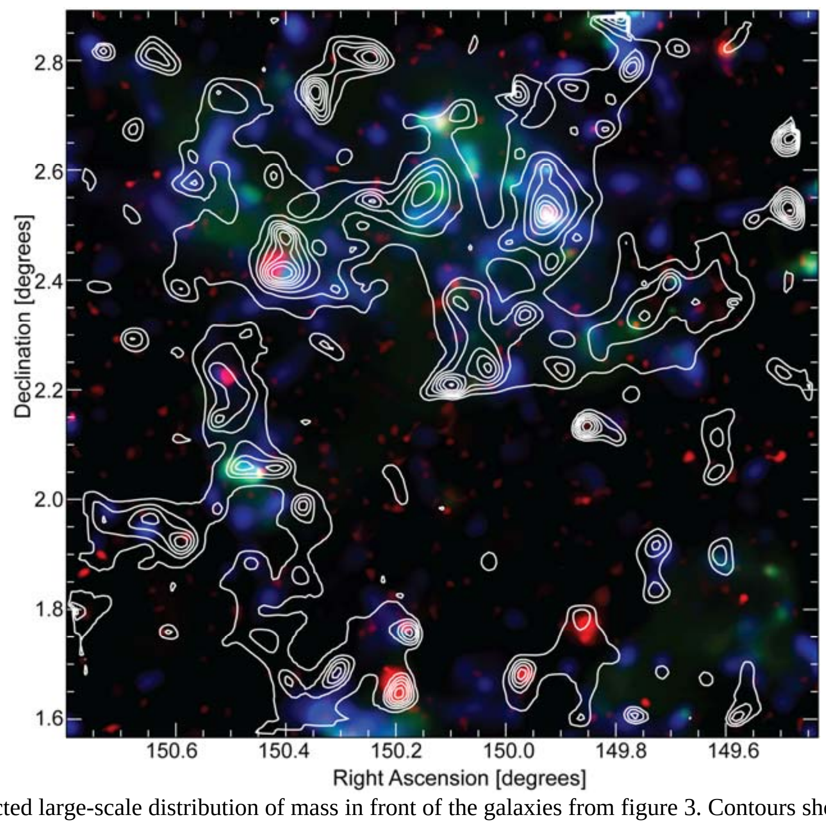

Fig. 4 The reconstructed large-scale distribution of mass in front of the galaxies from figure 3. Contours show the total distribution of mass, projected onto the plane of the sky. Like an ordinary optical lens, gravitational lensing is most sensitive to structures half-way between the source and the observer. The reconstruction is thus most sensitive to mass at redshift $z \approx 0.7$ and, to a lesser extent, all mass between redshifts 0.3 to 1.0. The various background colours depict different tracers of baryonic light. Green shows the density of optically-selected galaxies and blue shows those galaxies, weighted by their stellar mass from fits to their spectral energy distributions. These have both been weighted by the same sensitivity function in redshift as that inherent in the lensing analysis. Red shows X-ray emission from hot gas in extended sources, with most point sources removed. This is stronger from nearby sources, but weaker from the more distant ones. (Figure credit: Nature/R. Massey).

whether that is dominated by a recent major merger or gradual accretion of smaller subhalos. The particularly flat central concentration of mass in clusters could be explained by either a low level of interaction of dark matter particles through the electroweak force, or by partial free-streaming of “warm” dark matter away from the gravitational potential well. However, this picture is complicated by events from within the cluster, such as feedback, where the highly energetic explosions of massive stars purge material from the dense cluster core. Even dark matter can be affected by this, via the tidal gravitational influence of ejected baryonic material.

2.2 Individual galaxy clusters

A similar picture is obtained from reconstructions of the mass in individual galaxy clusters, which are all enveloped by a halo of dark matter. However, differences between the detailed distribution of baryonic and dark matter reflects their different interaction properties. For example, the inner core profile of the total indicates whether its construction was cominated by a single major merger, or gradual accretion of smaller subhalos. The particularly flat central concentration of mass observed in clusters could be explained by either a low level of (self-)interaction of dark matter particles via the weak force, or by partial free-streaming of “warm” dark matter away from the gravitational potential well. However, this picture is complicated by astrophysical processes and events within the cluster, such as feedback, where the highly energetic explosions of massive stars purge material form the dense cluster core. Even dark matter can be affected by this, via the dynamical gravitational influence of ejected baryonic material.

Another use of gravitational lensing mass reconstructions in individual clusters is to study the environmental dependence of galaxy formation and evolution. The 0.25 square degree HST STAGES survey covers the dense Abell 901/902 supercluster. A mass reconstruction of this, shown in figure 4, and that of the COSMOS field, act as a background tapestry on which the galaxies are painted. Studies of the properties of galaxies, as they transition from low density environments to high density clusters – undergoing bursts of rapid star formation and tidal stripping of gas – are ongoing.

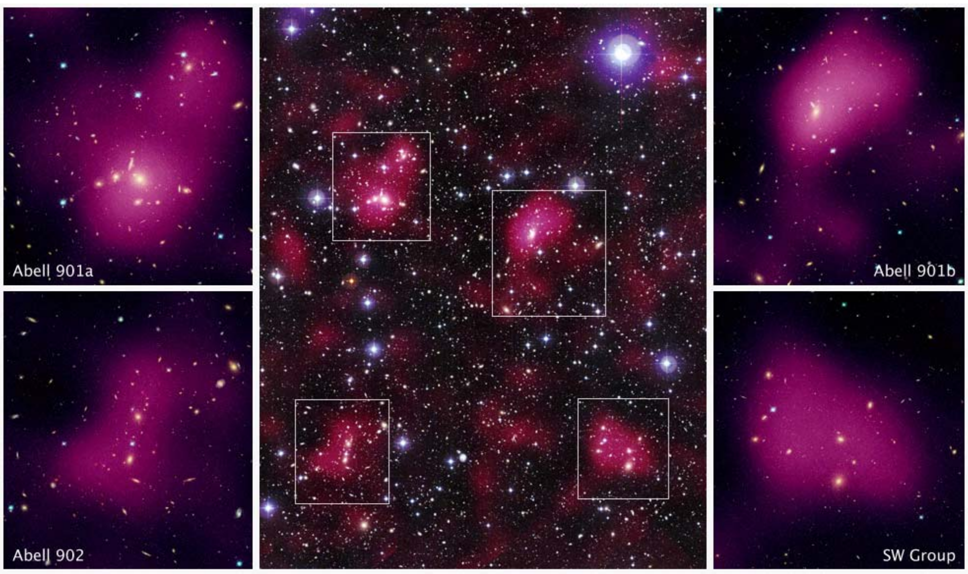

Fig. 5 The reconstructed distribution of mass in localized galaxy supercluster Abell 901/902, from the HST STAGES survey. The background image shows the distribution of galaxies, and the overlaid magenta shows the reconstructed distribution of mass. This targeted survey, containing extremely dense environments at a redshift ideal for measurements of gravitational lensing, will be useful to study the evolution of galaxies as they fall into the dark matter scaffolding. (Figure credit: NASA/ESA/C. Heymans/M. Gray).

2.3 The bullet cluster

Continuing to still smaller physical scales, the most interesting of all observed galaxy clusters is without doubt the "bullet cluster" 1E 0657-56, shown in figure 5. This provides the most direct evidence that the missing mass has very different properties to those of baryonic material. The bullet cluster is strictly two clusters that recently collided (about 150 million years ago), and we see the aftereffects of that collision. It is rather like the detritus ejected from a collision within a particle accelerator, and we can reconstruct the various ingredients of the original clusters from their subsequent trajectories. Individual galaxies within the clusters were initially well-spaced and had a very low collisional cross-section. Most continued moving during the collision, and today lie far from the point of impact. On the other hand, hot intra-cluster gas was uniformly spread throughout the incident clusters. This had a large interaction cross-section and – like a cosmic car crash – was slowed dramatically by the collision. The two concentrations of gas, seen in X-ray emission, have now passed through each other, but have not moved far from the point of impact. Interestingly, the collision speed and gas density were sufficient for a shock front to be observed in the gas from the smaller of the two clusters, allowing the determination of the collision speed.

A gravitational lensing reconstruction of the bullet cluster adds an additional ingredient to the original galaxy clusters. A great deal of mass is associated with the positions of the galaxies: around 30 to 40 times that in the form of stars and emitting visible light. Strong gravitational lensing observed around the dense

Fig. 6 The "bullet cluster" 1E0657-56. The background image shows the location of galaxies, with most of the larger yellow galaxies associated with one of the clusters. The overlaid pink feature shows X-ray emission from hot, intra-cluster gas. Both of these are associated with baryonic material. The overlaid blue shows a reconstruction of the mass from measurements of gravitational lensing. This appers conincident with the locations of the galaxies, implying it has a similarly small interaction corss-section. However, there is far more mass that that present in the form of stars within the galaxies, providing strong evidence for the existence of an additional reserve of exotic dark matter. (Figure credit: X-ray: NASA/CXC/CfA/ M.Markevitch et al.; Lensing Map: NASA/STScI; ESO WFI; Magellan/U.Arizona/ D.Clowe et al. Optical image: NASA/STScI; Magellan/U.Arizona/D.Clowe et al.).

cluster cores tightly constrains the position of these mass peaks, which are both in front of their corresponding gas peaks by more than 8σ. The additional mass clearly had a very low or zero collisional cross-section, but exhibits a usual gravitational influence – which implies that it consists of something with the same properties as those hypothesized for dark matter. Indeed, constraints on the collisional cross-section of dark matter incorporating the collisional speed derived from the X-ray shock front, rule out most of the proposed interaction cross-sections required to explain the flat mass profiles in cluster cores via even minimally self-interacting dark matter models.

The visible separation between the three ingredients of each cluster is only seen at this temporary moment in history. Within another billion years, the mutual gravitational attraction of the galaxies, gas and dark matter will have pulled them back together. They will spiral ever closer together until they resume the usual configuration of baryonic material within a larger dark matter cocoon.

One interesting controversy surrounding the bullet cluster has recently been resolved. The X-ray shock front naively suggests a collisional speed at the point of impact that would be a 5σ outlier in the range of speeds expected for such events: an unusually high figure to explain via individual peculiar motions. However, more recent calculations take into account the acceleration of the smaller cluster towards the larger and the relative motion of the gas clouds in the rest frame of the smaller cluster. With these calculations, the apparent velocity implied by the shock front is merely high but not unusal. Indeed, the shock front that led to the discovery of this object would not have been seen for a low-speed collision.

2.3 Individual galaxies

Gravitational lensing measurements can also be used to investigate the small haloes of dark matter around individual galaxies. This effect is so weak that the signal around many galaxies must be stacked. However, a consistent picture is emerging of a central density peak associated with the stellar mass, plus a larger halo of dark matter. Furthermore, this halo is most pronounced around older, redder galaxies.

3. Future opportunities

3.1 Interesting theoretical challenges

The interpretation of weak lensing measurements requires comparison either to the distribution of baryonic material or to theoretical predictions. Drawing constraints on parameters in any cosmological model certainly requires the latter. However, weak lensing measurements are typically made on relatively small physical scales. The weak lensing signal reflects the universe's matter power spectrum, and is strongest on small scales. However, the non-linear growth of structure in this regime is difficult to model in *n*-body dark matter simulations, because it is significantly affected by "gastrophysical" processes. Recent weak lensing measurements are becoming as precise as the current generation of theoretical models to which they are compared. If future error bars are not to be dominated by the inability of theories to predict the signal, advances in computational cosmological modelling must proceed apace.

The precise measurement of faint galaxy shapes, even from high resolution, space-based images, is a significant image analysis problem. Over the past decade, many methods have been developed to measure galaxy shapes, and correct them for the effects of convolution with the telescope's PSF. A recent collaboration between the global weak lensing community recently tested the performance of these methods on simulated astronomical images containing an artificial weak gravitational lensing signal. The Shear TEsting Programme (STEP) was run blind, so entrants did not know the input signal when they ran their methods. The achieved performance is of sufficient precision for current surveys, although far from perfect. Improvements are ongoing, although as larger surveys are obtained, with smaller statistical errors, significant advances will need to be made in image analysis techniques. A continuation of STEP has recently been launched, to gather expertise from the fields of statistical inference and computational learning. Indeed, entrants from all backgrounds are enthusiastically encouraged to the GRavitational lEnsing Accuracy Testing (GREAT08) 2008 Pascal challenge (www.great08challenge.info).

Very little work has yet focused on correcting the Charge Transfer Inefficiency of CCD detectors damaged by the harsh radiation in orbit, particularly from the perspective of weak gravitational lensing. Empirical calibrations have attempted to quantify the spurious changes in photometry, astrometry and shape measurement that are induced by the trailing of charge. Some pipelines have also been developed to take an imperfect, observed image then move charge back to where it belongs, pixel by pixel. This is the ideal approach, and should be the first step in an ideal data reduction pipeline since the trailing is created during CCD readout, the last process to happen on chip. However, current algorithms have concentrated on long trails from species of charge trap that mainly affect object photometry. It remains unclear how well such techniques can be applied to correct short trails that alter an object's shape.

3.2 Construction of dedicated spacecraft

To circumvent the atmospheric PSF, weak lensing measurements really need to be performed from a space-based observatory. The field has developed from a tentative idea to a mature subject with the Hubble Space Telescope. However, the current state of weak lensing measurements is rather like that of the CMB before WMAP: a series of measurements all roughly consistent, but showing only a hint of the high precision cosmology that could be possible. Aside from the instrumental problems of thermal variation and radiation damage, HST (and even JWST) is limited by its small field of view. The HST COSMOS mosaic of six hundred adjacent images maps one representative region of the sky, but in some sense is merely a proof of concept. Several efforts are proceeding in earnest to construct a dedicated observatory in space, with a much wider field of view. Located in high orbits, and designed for thermal stability with minimal radiation damage, these will map the entire sky at high precision, revealing our location in the much larger cosmic web, and directly track the statistical growth of structure in our expanding universe.

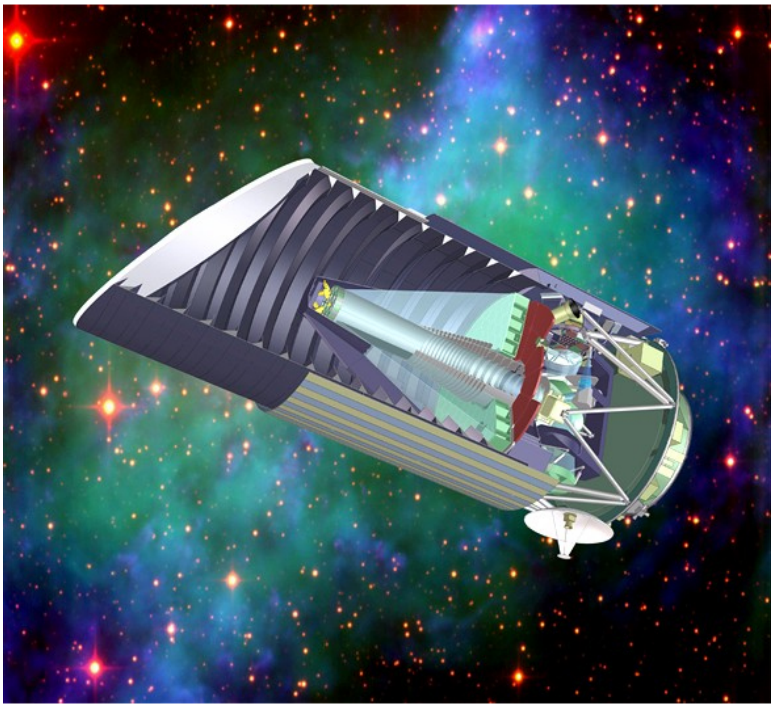

Fig. 7 Cutaway design view of the SuperNova/Acceleration Probe (SNAP), a candidate proposed for the NASA JDEM mission. This will feature a wide field of view, allowing it to, in principle, map dark matter across the entire sky and reveal our position in that giant cosmic web. Crucially, it will be placed in a high, thermally stable orbit, and the detectors are designed to be unaffected by radiation damage. It will therefore not suffer the main two problems that currently limit HST observations, and will be able to trace the growth of structure over cosmic time, plus the large-scale geometry of the universe, with unprecedented precision. SNAP will be to weak lensing what WMAP was to the CMB. (Figure reproduced courtesy of the SNAP team).

4. Conclusions

Weak gravitational lensing has long been postulated as a unique way to probe the large-scale gravitational fields of the universe, and serious attempts to detect it have been made since the 1980s. However, it was only with the advent of large-format CCD cameras around 2000 that the tiny signal was first detected. Indeed, the detection was so dependent upon technological innovation that four groups independently reported detections in that one year. Further recent progress in wide-field camera technology has rapidly advanced the field: in only eight years, weak gravitational lensing has become an accepted staple of cosmological tests, with detailed plans for dedicated missions in space. It represents a unique way to probe the distribution of mass in the universe, free of the usual reliance upon (often biased) tracers of electromagnetic radiation. Interesting challenges remain to be solved in theoretical computation, practical image analysis, and engineering design. Yet weak lensing appears to have a bright future as a mature astrophysical and cosmological tool.

References

Aldering G. et al. astro-ph/0405232 (2004)
Bradac M., et al., ApJ 652, 937 (2006)
Bridle S. et al., AOAS submitted, arxiv:0802.12.14 (2008)
Clowe, D. et al., ApJL, 648, 109 (2006)

Heymans C. et al., MNRAS 368, 1323 (2006)
Heymans C. et al., MNRAS in press, arxiv:0801.1156 (2008)
Kaiser N., Squires G. & Broadhurst T., ApJ, 449, 460 (1995)
Massey R. et al., MNRAS 376, 13 (2007)
Massey R. et al., ApJS, 172, 239 (2007)
Massey R. et al., Nature, 445, 286 (2007)
Refregier A., ARA&A, 41, 645 (2004)
Rhodes J., et al., ApJS, 172, 203 (2007)
Sand D., Treu T., Ellis R., Smith G. & Kneib, J.-P. ApJ, 674, 711 (2008)
Scoville N., et al., ApJS, 172, 38 (2007)
Schneider, P. 2005, Gravitational Lensing: Strong, Weak & Micro, Springer-Verlag, Berlin, 273.